sciendo

Polish Journal of Chemical Technology, 25, 3, 40—49, 10.2478/pjct-2023-0023

Influence of drying and granulation process conditions on the characteristics of micronutrient chelates granules

Bernard Michałek[1*], Katarzyna Bizon[2], Błażej Gierczyk[1], Tomasz Wilk[1], Magdalena Rapp[1]

[1]*Faculty of Chemistry, Adam Mickiewicz University, ul. Uniwersytetu Poznańskiego 8, 61-614 Poznań, Poland*
[2]*Faculty of Chemical Engineering and Technology, Cracow University of Technology, ul. Warszawska 24, 31-155 Kraków, Poland*
[*]*Corresponding author: e-mail: bernard.michalek@adob.com.pl*

Fluidized-bed spray granulation (FBSG) enables manufacturing particles with desired characteristics, including particle size distribution (PSD), density, or dust content. This study investigated the effect of selected factors on the granules obtained in a continuous FBSG of chelated fertilizers for foliar applications. The effect of surfactant addition to the solution sprayed into the bed and perturbations of operating parameters on PSD and granules morphology was studied. The experiments were supplemented with calculations based on a population balance equation (PBE). It was shown that granules manufactured with the tenside addition are more regular in shape, and thus less prone to mechanical wear. It was demonstrated that increasing rotational mill speed does contribute to a slight increase in the amount of dust, but in the long term, it does not disturb the regular agglomeration process. The computational results confirm that, despite the complexity of the process, its description with PBE is feasible.

Keywords: fluidized bed spray granulation, chelate granules, surfactants, population balance modelling, granule morphology.

INTRODUCTION

Fluidized-bed spray granulation (FBSG), also referred to as wet granulation enables solutions, suspensions, or melts to be converted into coarse-grained, dust-free, and easy-to-handle granules. In the FBSG the liquid is sprayed into or onto a bed made of particles that are fluidized by a stream of hot drying gas inducing particles (tablets, granules) enlargement[1]. Depending on the material properties and adopted process conditions, this enlargement occurs through layering or agglomeration. Both mechanisms can take place in parallel, but only one should prevail, given the end use of the granular product[2]. The granulation process is usually accompanied by a number of antagonistic phenomena such as attrition or particle breakage[3].

Nowadays, FBSG is widely implemented in such areas as pharmaceutical, food, agricultural and chemical industries[1, 4–5]. Its popularity results mainly from the fact that through fluidized-bed granulation, desired particle or product characteristics can be achieved, such as porosity, particle size distribution (PSD), bulk density, dust content, and solubility. In addition, since the liquid sprayed on the solids can contain various additives, active substances, or nutrients, the added value of the granule can be easily gained. This feature is particularly important in the manufacturing of pharmaceuticals products, foodstuffs, detergents, or fertilizers[5].

Despite the extremely wide range of industrial applications and the relatively mature character of this technology, FBSG units still face significant challenges for both experimenters and modelers. The enormous complexity of the FBSG process arising, among other things, from the three-phase nature of the flow and from closely coupled phenomena of heat and mass transfer contributes to the numerous difficulties associated with the successful operation of FBSG units. Even some recent works[6–7] indicate that there are still enormous literature gaps, and consequently a lack of theoretical and practical knowledge inherent in FBSG technology. In this context, one can mention the lack of complete knowledge about the influence of the binder/sprayed formulation on the agglomeration rate or the lack of assessment of scalability of mathematical models. The latter flaw translates into major problems in the optimization and control of industrial units and difficulties in early detection of failures, for example, uncontrolled agglomeration arising from a phenomenon termed wet quenching[8].

A thorough understanding of the process is indispensable for the development of a methodology for obtaining granules with the required properties, such as sufficiently narrow size range, porosity, bulk density, and composition. One of the paths towards achieving the right quality of granules is proper control of wetting during the process. This can be accomplished, for example, by adding the right amount of surfactant to the formulation sprayed onto the bed or by altering, either by means of additives or by changing the ratio of dissolved solids, its viscosity[9]. The first approach is particularly attractive for the production of granular foliar fertilizers such as various micronutrient chelates of Mn, Zn, Fe based on IDHA, i.e. iminodisuccinic acid[5]. The addition of surfactants not only affects the kinetics and hydrodynamics of the manufacturing process itself but also facilitates the penetration of micronutrients into the waxy leaf surface[10, 11], and has the potential to both increase the wettability of the leaf surface and determine the direction of spread of fertilizer droplets[11].

As mentioned above, the huge number of factors conditioning the entire FBSG process, and thus the quality of the granules obtained, is up to now still a major problem. The most important of these include (Fig. 1): the design of the apparatus itself, the materials used, the process conditions adopted, as well as the measurement and computational procedures supporting the control of the actual process.

For instance, there is an extremely close relationship between the FBSG unit design and the properties of the materials used and, additionally, the process conditions adopted. The size of the droplets and their distribution is intrinsically related to the type of nozzles used and

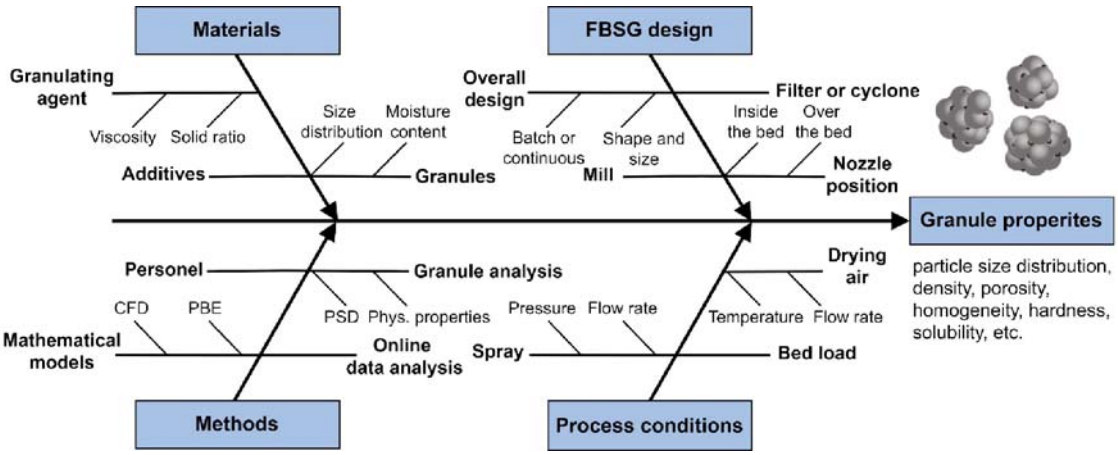

Figure 1. Ishikawa diagram indicating parameters and factors affecting granules properties

their arrangement in the apparatus, i.e. inside or above the fluidized bed. The wetting and drying mechanisms, and consequently also the agglomeration, are closely related to the physicochemical properties of the liquid formulation, such as its composition and viscosity, and to the temperature and flow rate of the drying gaseous medium. The fluidization velocity determines the hydrodynamics of the bed, and thus also the intensity of phenomena antagonistic to granule enlargement such as fragmentation or attrition[12], significantly affecting the particle size distribution in the bed. The latter requires particular attention, especially in the case of continuous processes, where to maintain steady-state conditions, one seed particle must be formed by nucleation or must be added to the system for each product particle removed[13].

Another factor influencing the efficiency of the granulation process and therefore the final granule properties is the broadly defined methodology (methods) (Fig. 1), which includes all online and offline process monitoring techniques, together with human factors and automatic control systems or computational tools. It needs to be underlined here that mathematical modelling, optimization, and control of FBSG processes remain also in demand to refine existing or develop new computationally affordable mathematical and simulation tools[6–7]. Regardless of the operation mode of the process, i.e., continuous or periodic (batch), the modelling of granules size enlargement can be performed employing various approaches, ranging from the most popular macroscopic description based on population balance equation (PBE)[1, 9, 14], to the discrete element method coupled with computational fluid dynamics (CFD-DEM)[15]. The development of a computational methodology that might be implemented for model predictive control (MPC) of FBSG processes or for fault detection (e.g. wet quenching), and therefore implementable online (i.e. for real-time calculations), definitely requires a focus on a simplified description of the granulation process based on PBE approach. However, PBE-based methodology needs to be revisited and augmented with all relevant elements and phenomena that are usually neglected, for instance, phenomena antagonistic to granulation.

Considering the above-described concerns and knowledge gaps this study provides an overview of the influence of selected factors on the characteristics of granulated chelates together with some findings on the process modeling based on PBE approach. Since one of the factors significantly affecting the drying process and the granulation itself are various additives, the effect of the addition of polyglucoside surfactants and betaines to the fertilizer solution sprayed into the fluidized bed during the production of *N*-(1,2-dicarboxyethyl)-D,L-aspartic acid disodium zinc salt by PPC ADOB was analyzed. In particular, the effect of surfactant addition on the granule size distribution during the continuous operation of the apparatus operation was studied. Furthermore, the effect of changes in the selected operating parameter, namely the rotational speed of the mill, on the stable process was analyzed. In addition, using the experimental results, the parameters of the continuous process model based on PBE approach were determined.

MATERIALS AND METHODS

Experimental

An FSBG pilot installation shown schematically in Fig. 2 was used to conduct the process of microelement chelate agglomeration of *N*-(1,2-dicarboxyethyl)-D,L--aspartic acid disodium zinc salt. In such an installation, the process of liquid spraying and granulation takes place in a single volume. The granulated and dried fraction is continuously collected from the fluidized bed, and subsequently, the solid mixture is segregated on a sieve where the granulate fraction of the target product is collected outside the test system. On the other hand,

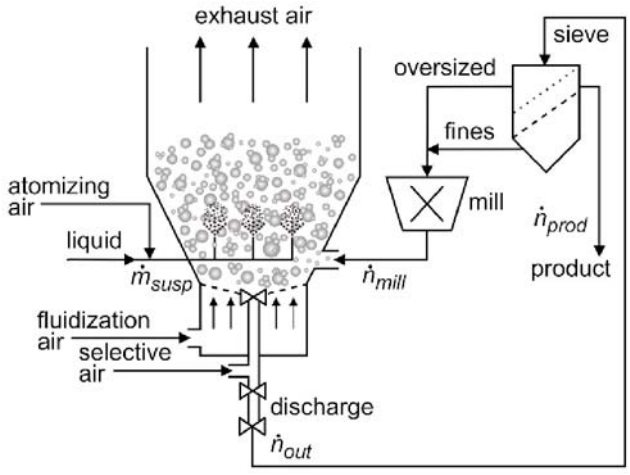

Figure 2. Scheme of a continuous FBSG pilot installation with external product separation and milling

dust and oversize granules are returned after grinding into the fluidized bed in order to initiate the process of nucleation, consolidation, and agglomeration. The ADOB-specific type of dryer used for this experiment was AE3B17143.

As a first step, the effect of the addition of polyglucoside surfactants and betaines to the fertilizer solution sprayed into the fluidized bed during the production of microelement chelate was analyzed. Then, during the experiment conducted for microelement chelate granulation with the tenside addition, the rotational speed settings of the mill was raised by about 15%. For each of the settings, the duration of the experiment was up to 8 hours, during which samples were taken at equal time intervals and then protected against the influence of weather conditions.

The FBSG process was carried out based on the internal procedure of the ADOB company. The so-called steady state was maintained throughout the test and sampling period. It means that fluidized bed pressure drop and inlet temperature remained constant for a time corresponding to the value of mean residence time of particles, τ:

$$\tau = \frac{m_{fb}}{\dot{m}_{susp}\, x_{solute} + \dot{m}_{nuclei,ext}} \tag{1}$$

with liquid feeding and product outtake also being constant. The mean residence time of solid particles calculated by Eq. (1) resulted to be τ = 2119 s where m_{fb} is fluidized bed mass, $\dot{m}_{susp}$ is mass flux of suspension fed into the drying zone, x_{solute} is suspension dry mass and $\dot{m}_{nuclei,ext}$ is external nuclei mass flux ($\dot{m}_{nuclei,ext} = \dot{m}_{mill}$).

Granule samples for analysis were collected from the fluidized bed just above the gas distributor under the established process conditions for which stability of the fluidized bed was achieved The mixture of particles was analyzed with regards to particle size ranges using sieve analysis and image analysis. The analysis was conducted with a Retsch AS 200 analyzer using a vibration amplitude of 60% (digital, 1–100%; 0–2 mm) and using an automated particle characterization tool Malvern Morphologi G3. The size and shape parameters of the granules obtained with and without tenside addition were evaluated, and a static microscope image analysis was made to assess the nature of the bed material and fine fraction recycled from the mill. Additionally, based on the relevant standards[16–18], the effect of tenside addition on the specific, bulk density and specific surface area of solid particles obtained in a continuous process were determined (Table 1).

Process modelling

The general form of the population balance equation (PBE)[19–21] for a well-mixed system operating in a continuous mode and assuming (Fig. 2) that withdrawn granules, $\dot{n}_{out}$, are sieved into three fractions, i.e. the product that is removed from the system, $\dot{n}_{product}$, the oversized particles, , and fines, $\dot{n}_{fines}$, with the latter two classes being returned to the granulator after milling, $\dot{n}_{mill}$, can be written as follows:

$$\frac{\partial n}{\partial t} = \dot{n}_{growth} + \dot{n}_{agg} + \dot{n}_{mill} + \dot{n}_{nuc,int} - \dot{n}_{out} \tag{2}$$

where n is the population density based on the total number of granules in the bed, $\dot{n}_{growth}$ is their growth due to layering and $\dot{n}_{agg}$ denotes granules size enlargement by agglomeration, and $\dot{n}_{nuc,int}$ refers to internal nucleation by overspray and attrition.

The growth rate due to the coating and solidification of successive layers of suspension sprayed onto the bed, $\dot{m}_{susp}$, usually is assumed to be size independent and is expressed as[20]:

$$\dot{n}_{growth} = -G\frac{\partial n}{\partial L} \quad \text{where } G = \frac{2\left(1-x_{liq}\right)\dot{m}_{susp}}{\rho_{solute}A_{p,tot}} \tag{3}$$

where x_{liq} denotes the moisture fraction in the suspension sprayed into the bed with the mass flow rate, $\dot{m}_{susp}$, ϱ_{solute} is the solute density and $A_{p,tot}$ is the total surface of particles.

Some of the droplets dry before hitting the surface of the granules present in the bed, contributing to nucleation, which yields the following modification[20] of Eq. (3):

$$G = \frac{2\left(1-b\right)\left(1-x_{liq}\right)\dot{m}_{susp}}{\rho_{solute}A_{p,tot}} \tag{4}$$

where b denotes the spray fraction contributing to nucleation via overspray, i.e. spray-dried droplets. The nucleation term due to overspray can be expressed as[20]:

$$B_{overspray} = \frac{6b\left(1-x_{liq}\right)\dot{m}_{susp}}{\pi L_0 \rho_{solute}}\delta\left(L-L_0\right) \tag{5}$$

where L_0 denotes the nuclei diameter and δ is the delta function.

A further modification of Eq. (3) and (4) can be made to include the attrition mechanism in the internal nucleation term[22], $\dot{n}_{nuc,int}$, since this antagonistic to particle enlargement phenomenon influences also the rate of diameter change, G. This results in the term associated with internal nucleation to consist of two elements, i.e. overspray and attrition, $\dot{n}_{nuc,int} = B_{overspray} + B_{attrition}$.

The agglomeration term, $\dot{n}_{agg}$, is described following the model[23] expressed in relation to the particle size L, represented in this study by particle diameter, d, as:

$$\dot{n}_{agg} = B_{agg} - D_{agg} \tag{6}$$

$$B_{agg} = \frac{L^2}{2}\int_0^L \frac{\beta\left(\left(L^3-\lambda^3\right)^{1/3},\lambda\right)\cdot n\left(\left(L^3-\lambda^3\right)^{1/3},\lambda\right)\cdot n(\lambda)}{\left(L^3-\lambda^3\right)^{2/3}}d\lambda \tag{7}$$

$$D_{agg} = n(\lambda)\int^{\infty}\beta\left(L,\lambda\right)\cdot n(\lambda)\,d\lambda \tag{8}$$

where λ is the variable of integration and $\beta(L, \lambda)$ is the coalescence kernel, containing information about the probability of forming new agglomerates. In general, it is the product of two contributions[24], i.e. the aggregation rate constant, $\beta_0(t)$, and a particle-size dependent term $\beta^*(L_x, L_y)$. Based on the previous study concerning the batch granulation process of fetilirizers[5], an equipartition kinetic energy[24] (EKE) kernel was used in this study to describe the particle-size dependent term:

$$\beta^*\left(L_x,L_y\right) = \left(L_x + L_y\right)^2\sqrt{\frac{1}{L_x^3}+\frac{1}{L_y^3}} \tag{9}$$

Moreover, given the continuous nature of the process, the time dependence of the kernel was neglected resulting in $\beta_0(t) = \beta_0$.

The granule flux being removed from the FBSG, $\dot{n}_{out}$, can be described using the formula[21]:

$$\dot{n}_{out} = Kn \tag{10}$$

with K being removal rate, accounting usually for the classifying character of the outlet[25]. The classes into which the removed granules, $\dot{n}_{out}$, are classified after screening are[22]:

$$\dot{n}_{fines} = (1-T_2)(1-T_1)\dot{n}_{out} \tag{11}$$

$$\dot{n}_{product} = T_2(1-T_1)\dot{n}_{out} \tag{12}$$

$$\dot{n}_{oversize} = T_1\dot{n}_{out} \tag{13}$$

In the ideal case, it can be assumed that T_1 and T_2 are the Heaviside functions:

$$T_{1/2} = H(L - L_{1/2}) \tag{14}$$

where, in the analyzed here case, L_1 = 900 μm and L_2 = 200 μm.

Taking into account that both the oversize granules and fines are then transferred to the mill (Fig. 2), the flux of granules subject to milling, $\dot{n}_{mill,inlet}$, is:

$$\dot{n}_{mill,inlet} = (1-T_2+T_1)\dot{n}_{out} \tag{15}$$

Since milling is a complex process, and in this case the effect is even more complex because fines also pass through the mill, to evaluate the flux of particles fed back to the granulator a particle number density function determined experimentally, $\dot{m}_{solute}$, was employed.

Assuming ideal mass control, it is possible to calculate the drain value, K, in Eq. (10), which is required to maintain a constant bed inventory during the continuous operation mode of the FBSG. Keeping in mind that in a steady state $\partial n/\partial t = 0$ and thus also $\partial m/\partial t = 0$, with m being the mass, analysis of the scheme shown in Fig. 2 and the PBE given by Eq. (2), indicates that the dry mass injected into the granulator per unit time, $\dot{m}_{solute}$, must be equal to the mass flow rate of the product, $\dot{m}_{prod}$, resulting in the following equality:

$$(1-x_{liq})\dot{m}_{susp} = \dot{m}_{solute} = \dot{m}_{prod} \tag{16}$$

Assuming further uniform solid density and that particles are spherical in shape the above formula can be rewritten as:

$$\dot{m}_{solute} = \frac{\pi}{6}\rho_{solute}\int_0^\infty L^3 T_2(1-T_1)KndL \tag{17}$$

Given the nature of the experimentally determined particle size distribution with negligible amount of fines (refers to the tests with tenside addition only), all granules were assumed to have the same probability of leaving the apparatus through the drain, which yields:

$$K = \frac{\dot{m}_{solute}}{\frac{\pi}{6}\rho_{solute}\int_0^\infty L^3 T_2(1-T_1)ndL} \tag{18}$$

This means that the only parameter that needs to be identify based on the experimental data is the agglomeration constant in the coalescence kernel, β_0. The parameter estimation was conducted in Matlab by minimizing the sum of squares of the residuals between the PSD calculated using the discretized PBE, following the discretization methodology proposed in the literature[19, 23], and the experimental PSD. The parameter estimation procedure was implemented with the use of *fminsearch* function with an embedded *fsolve* function.

RESULTS AND DISCUSSION

In a previous study[5], it was demonstrated that the addition of surfactant to the solution sprayed into the bed increases granulation kinetics during batch operation of a FBSG and that the mechanism of agglomeration prevails over the mechanism of layering. The addition of surfactant not only lowers the surface tension, but also increases the ability of successful granule aggregation due to the longer-lasting sticky surface of the granules. The latter effect is due to the altered final stage of water evaporation from the solution containing tenside. Given that the manufacturing process of granular fertilizers is usually carried out in a continuous mode, this study focuses on the properties of granules obtained from such a process.

Figure 3 shows a comparison of the volume, q_3, and number, q_0, density distributions of granules collected during a stabilized continuous process carried out without and with the addition of surfactant and determined using automated image analysis (Malvern Morphologi® G3). The results shown in Fig. 3 refer to the target product, i.e., the sample from which the oversize (> 0.9 mm) and

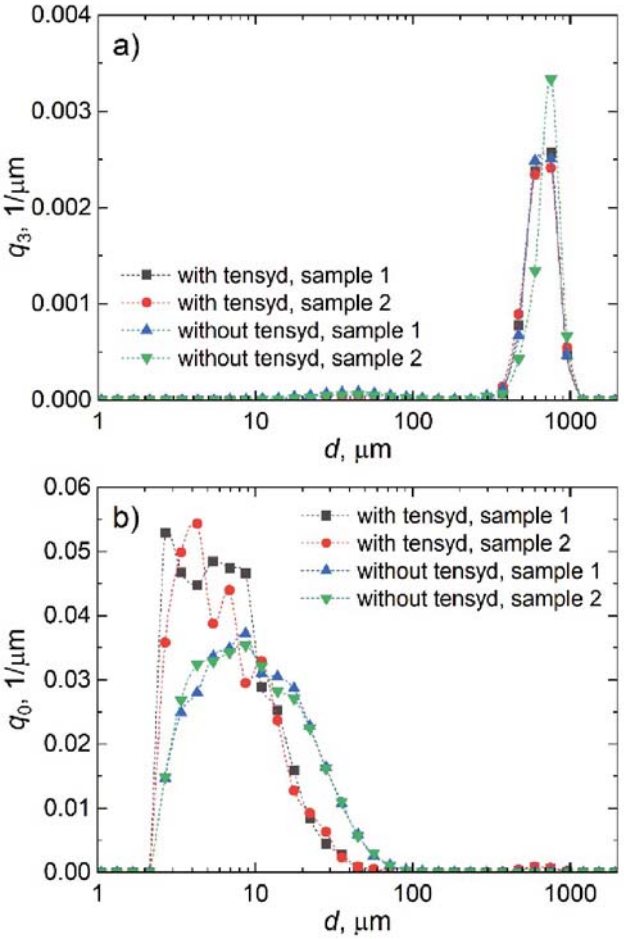

Figure 3. Volume, q_3 (a) and number, q_0 (b) density distributions of the target product fraction obtained during the test conducted with and without tenside addition

undersize (< 0.2 mm) granules were separated within the FBSG installation ($\dot{n}_{out}$ flux in Fig. 2).

Despite the product screening, the volume distributions of the product obtained without the addition of tenside (Fig. 3a) are bimodal in nature, with a second slight peak in the curve between the diameter range of about 10 to 100 μm. This indicates a non-negligible, in terms of volume/mass, fraction of granules within this diameter range in the final product. Their presence is even more evident on the number density distribution shown in Fig. 3a. The q_0 curves obtained for samples without tenside are shifted clearly to the right, i.e. toward larger diameters (i.e. coarser dust), compared to samples obtained with tenside. While the presence of fines in the product may be justified by abrasion of the surface of the granules, e.g. at the stage of transport and storage, the observed here difference in PSD indicates the existence of additional factors. Indeed, the conducted imaging analysis of the granules reveals differences in the outer surface of the granules obtained in the process with and without the tenside addition (Fig. 4). While the sample of the final product manufactured with tenside contains almost no fines resulting from abrasion (Fig. 4b and 4d), coarser dust is present in the sample from the test run without tenside (Fig. 4a). This is likely to be the result of a different surface structure. The surface of granules obtained with tenside is relatively smooth (Fig. 4d), which is the result of better spreading of the solution on their surface before solidification and more plastic surface during the granulation stage. On the other hand, the contour of the projection of the granule without tenside (Fig. 4c) is characterized by high irregularity. Such an irregular surface contributes to the tendency to form coarser dust particles.

The greater amount of dust in the product obtained without tenside is also reflected in the average granule diameters determined by averaging the results obtained from three measurements performed using automated image analysis, both for granules manufactured with and without tenside. The median granule diameters, d_{50}, by volume (q_3, Fig. 3a) are, respectively, 751.3 and 754.4 μm for particles produced without and with the addition of tenside. The d_{50} of the number distributions (q_0, Fig. 3b) are also relatively close to each other and are 19.4 μm (without tenside) and 16.5 μm (with tenside addition). However, analysis of the Sauter diameter, d_{32} (calculated for q_3) and the arithmetic mean diameter, d_m (calculated for q_0) indicates a decrease in these values when there was no surfactant added to the suspension sprayed into the bed. These values are, respectively, for the product obtained with and without the addition of tenside, d_{32} = 725.7 μm and d_m = 214.4 μm, and d_{32} = 667.9 μm and d_m = 38.6 μm.

To further explore the effect of tenside addition, its impact on the morphological parameters of the granules obtained in the test drying after obtaining the stable state of the fluidized bed was evaluated. In particular, with the use of Malvern Morphologi® G3, the circularity and concavity of the granules were determined.

Figure 5 shows the evolution of morphological parameters as their diameter increases determined for samples collected directly from the bed (without prior sieving). The results presented here are average values calculated from three measurements. The individual measurements provided consistent results. A clear impact of tenside addition on the

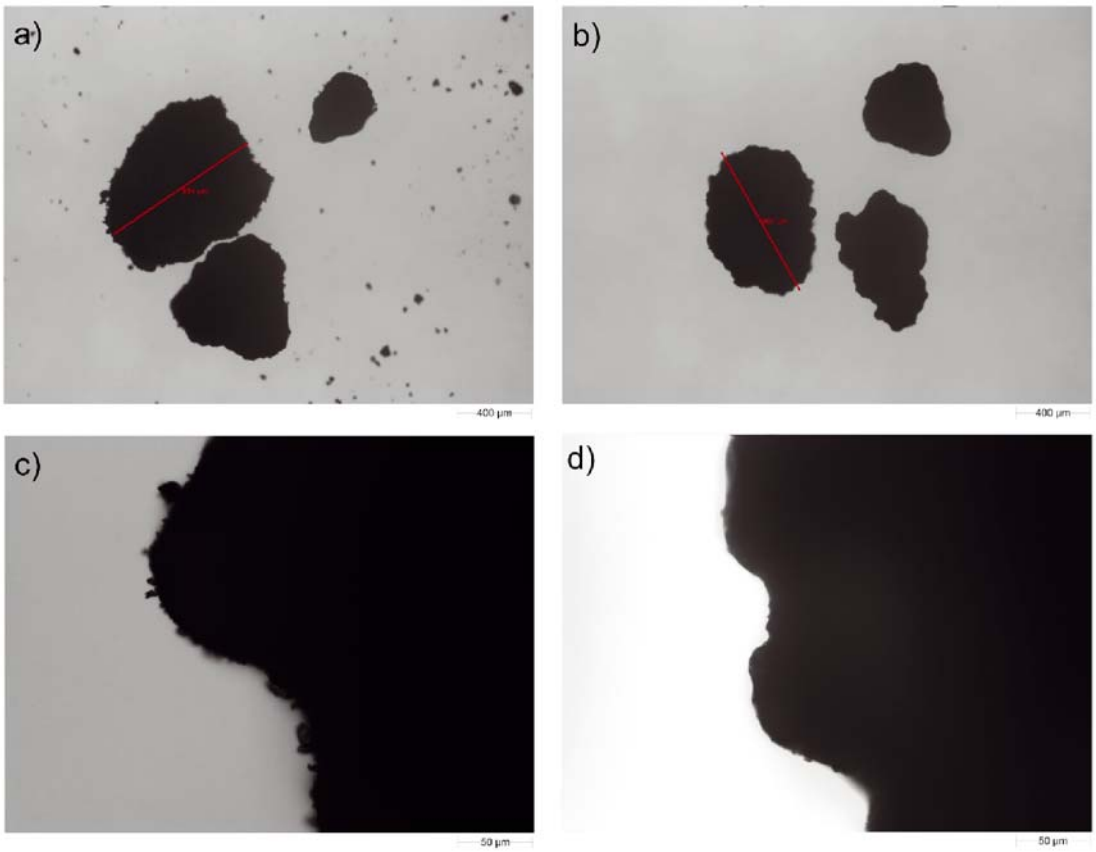

Figure 4. Representative particles sampled from the final product, i.e. from the fraction with a diameter range of 0.2–0.9 mm, manufactured without the addition of surfactant (a) and (c), and with its addition: (b) and (d)

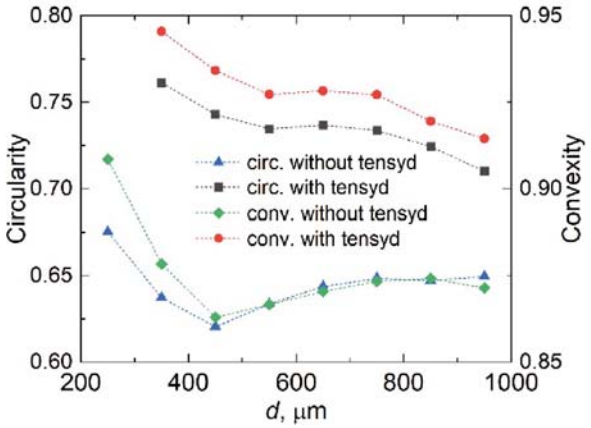

Figure 5. Evolution of the shape parameters with granule enlargement determined for the material sampled directly from the fluidized bed

granules circularity and convexity can be observed, which in the same fraction sizes are larger than those of granules without tenside. The latter have more irregular and less circular shapes, which may be related to a greater tendency for abrasion, breakage of granules during the agglomeration process or their degradation during pneumatic transport.

The decrease in the values of morphological parameters with increasing diameter of granules manufactured with tenside is due to their lower tendency to abrasion and greater tendency to growth by agglomeration than by layering. This, as a result, leads to the formation of raspberry-like granules. While the mechanism of growth by agglomeration also predominates in the case of granules produced without the addition of tenside, their greater tendency to abrasion implies that: (1) mainly larger granules are exposed to this phenomenon, hence the increase in the values of morphological parameters with the increase in diameter (from about 450 µm); (2) the presence of a relatively large amount of dust in the dryer chamber causes the suspect that one of the mechanisms affecting the growth – especially of larger granules – might be also the dust integration[26]. In both cases, the smallest fractions characterized by the highest values of circularity and convexity correspond to granules resulting from effects antagonistic to granulation (e.g., breaking or mechanical grinding in the mill) and granules formed primarily as a result of layering on the nuclei.

There is also a visible influence of the addition of tenside on the specific density (Table 1) of granules obtained in the continuous drying and granulation process which is generally lower for granules with tenside. This may be due to the foaming effect when spraying using a nozzle (two fluid nozzle). The foaming also likely affects the higher specific surface area values of granules prepared with the addition of tenside to the solution (Table 1).

As demonstrated above, the surfactant additive implies variations in the micronutrient chelate granule morphology, which in turn is closely related to antagonistic to granulation phenomena and therefore also to nucleation processes. In addition to internal nucleation promoted by abrasion and overspray, dust recirculation is a very important element for process continuity. For this reason, in the next stage of the study, the focus was on the nucleation process.

Figure 6 shows a comparison of the volume density distributions derived by means of image analysis for a sample collected directly from the bed, a sample collected from the mill and a sample of the sieved product (0.2 mm < d < 0.9 mm). These samples were collected during a stable process conducted with the tenside addition. The values of mean diameters calculated from the PSDS shown in Fig. 6 are respectively: d_{32} = 777.5 µm and d_m = 757.8 µm (bed material), d_{32} = 674.5 µm and d_m = 608.1 µm (sieved product), d_{32} = 176.2 µm and d_m = 122.5 µm (material sampled from the mill). Zooming in the plot for diameters below 100 µm confirms previous conclusions about abrasion occurring in the final product (anyhow, due to the use of tenside, this effect is here negligible). Of particular interest, however, is the shape of the distribution of particles originating from the mill. It is suspected that the first rather smooth part of the PSD curve (up to $d \approx 40$ µm) is related to the dust particles that enter the mill along with the oversize granules.

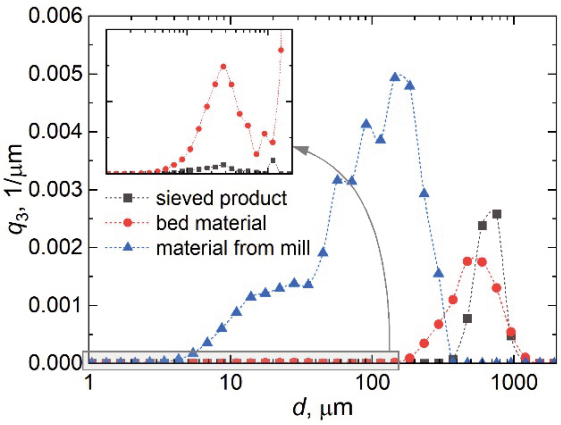

Figure 6. Volume density distributions of the sieved (target product) material, bed material and material sampled from the mill. Granules obtained with tenside addition

The second part of the distribution is strictly a consequence of the milling operation. This conclusion is confirmed by some visual observations of the granules shown in Fig. 7. In the material collected from the mill (Fig. 7c and 7d), it is possible to observe both relatively large particles with irregular shapes and sharply cut surfaces (Fig. 7d), as well as, for example, dried drops of overspray (Fig. 7c), which are formed earlier in the phase of spraying of the solution into the fluidized bed (Fig. 7a).

To further investigate the impact of the mill and dust recirculation on the entire process, during the experiment conducted for microelement chelate granulation with the tenside addition, the rotational speed settings of the mill was raised by about 15%. Figure 8a shows the effect of increasing the mill rotational speed on PSDs, determined here by both sieve and image analysis. Comparison of the distributions (Fig. 8a) with those obtained from a stable process run at lower rpm (Fig. 6), reveals that increasing the grinder rotation speed significantly influences the PSD

Table 1. Density and specific surface of the granule obtained in the test without and with addition of the tenside

Sample	Specific density, g/cm^3	Average bulk density, g/cm^3	BET MP, m^2/g	BET SP, m^2/g
Without tenside	2.031	0.82	0.153	0.122
With tenside	1.861	0.71	0.275	0.245

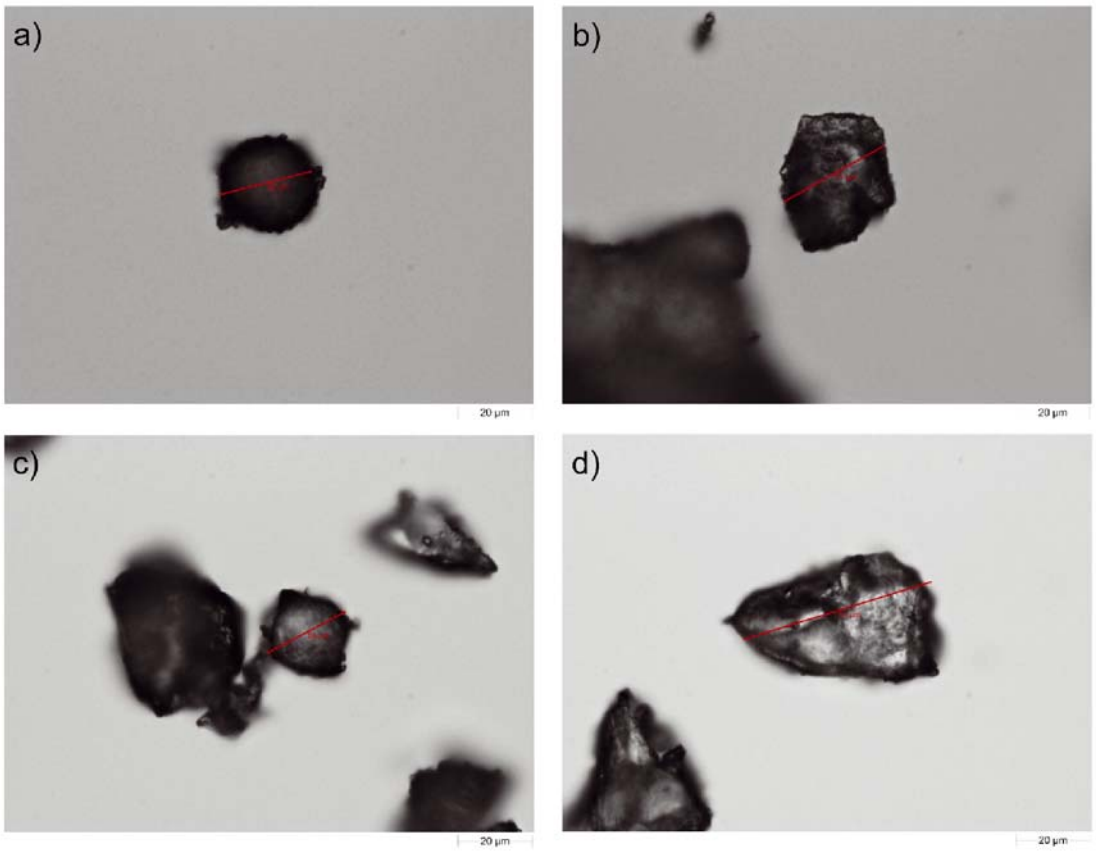

Figure 7. Fine particles found in the material sampled from the fluidized bed (a)–(b) and in the material sampled from the mill (c)–(d). Granules obtained with tenside addition

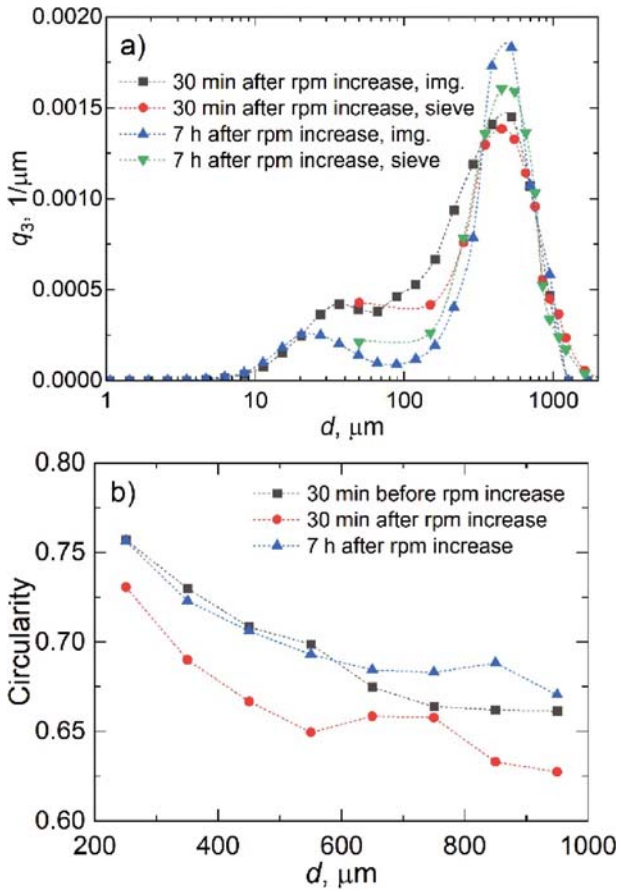

Figure 8. Volume density distributions of the bed material sampled 30 min and 7 h after increasing the rpm of mill (a), and influence of the milling of the shape parameters of granules (b). Granules obtained with tenside addition

in the fluidized bed. After changing the mill setpoint to a higher rotational speed, the concentration of larger particles (0.2–1 mm) drops and concentration of fine fraction increase. It should be noted that in the initial phase (curves corresponding to 30 min after increasing the rpm in Fig. 8a) there is a significant increase in the fractions with a diameter range between 40–100 µm, which, as previously mentioned, are typical outcome of the grinding effect. These contribution drops again after the process stabilizes (7 h after increasing the rpm in Fig. 8a), but remains at a slightly higher level than it was for the process conducted at lower mill rotations (Fig. 6). According to mass distributions obtained from sieve analysis the mean particle size d_{50} of granules involved in the process show slightly decrease after the rotor speed was increased, from 585 µm to 539 µm. Increasing the mill rotational speed and thus increase in the comminution of the returned fraction also results in changes in the morphological parameters of the granules such as circularity or convexity (Fig. 8b and 9). However, these parameters also go back to their previous level after some time. Therefore, the greater fragmentation of the returned fraction promotes agglomeration without disturbing the steady state under stable operation mode. Note, that increased fine fraction may increase nucleation tendencies, and thus in a situation of excess dust, dust deposition on the walls of the apparatus could be expected, however, no such phenomenon was observed. Considering these factors, higher mill settings can be considered more favorable.

The final part of the work involved solving the population balance equation (PBE) while using experimental data to fit the model, in particular to determine the

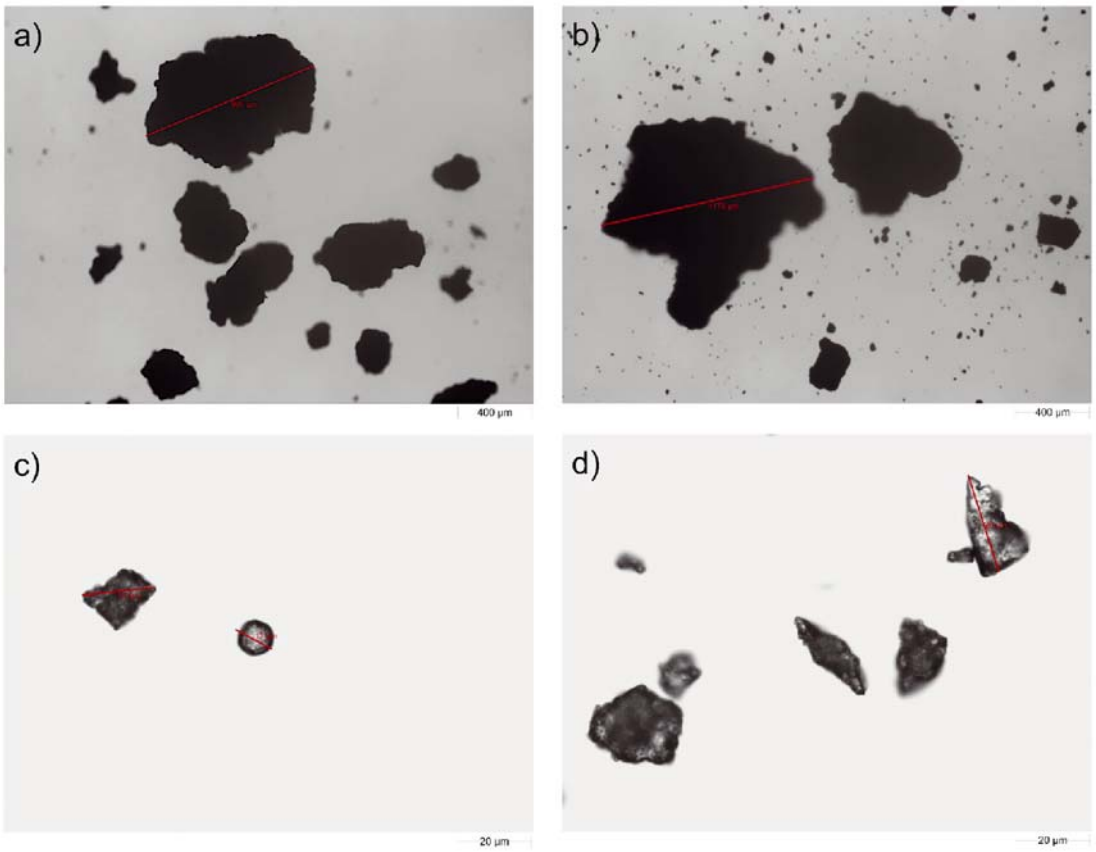

Figure 9. Particles sampled from the fluidized bed before (a) and (c), and 30 min after (b) and (d) increasing the mill rpm. Granules obtained with tenside addition

value of coalescence kernel, β_0. The drain rate, K, was calculated on the fly, internally within the optimization procedure, from the formula given by Eq. (18). Details on PBE discretization can be found in the literature[19, 23], and in the previous study[5]. Due to the complexity of the grinding process, an experimentally determined PSD was used to describe the particle flux leaving the mill. In addition, due to the small amount of overspray in the samples analyzed and because of the impossibility of estimating its actual contribution, the nucleation caused by this mechanism was neglected thus giving $b = 0$.

Before analyzing the model results, it is worth to examine the separation (screening) functions (Eq. (14)) effect on the distribution of granules in the flux leaving the apparatus, $\dot{n}_{out}$ (Fig. 10). Due to ideal mixing and adopted here assumption that all granules have the same probability of leaving the apparatus through the drain, this distribution is equivalent to the distribution of particles in the fluidized bed. Ignoring the influence of the classifying air on the distribution of the removed particles seems reasonable only in case of negligible amount of fines present in the bed when the process is run with tenside addition. Moreover, a comparison of the shape of the size distribution of granules in the bed in the range of small diameters (~5–70 µm) with the size distribution of particles from the mill suggests that the presence of this fraction in the latter may be the result of the abrasion described earlier, occurring in the plant already after sieving, or is the result of cohesion forces. In the latter scenario, the fines can adhere to larger granules in the bed and leave the apparatus even at classification air velocities much higher than their terminal velocity. This is also confirmed by the previously described presence of overspray in samples taken from the mill (Fig. 7c).

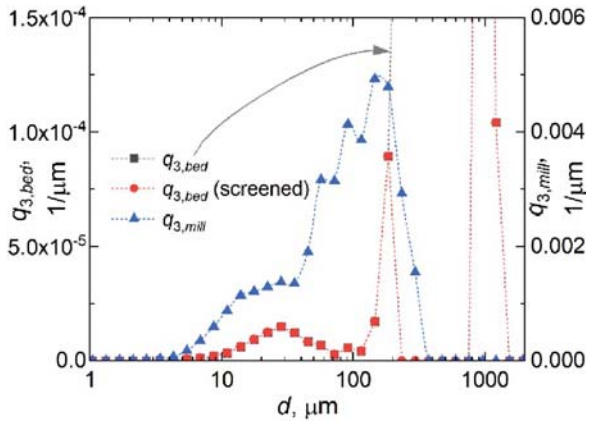

Figure 10. Effect of separation functions $T1$ and $T2$ on the volume density distribution of the bed material, $q_{3,bed}$, compared to the distribution of the particles sampled from the mill, $q_{3,mill}$. Granules obtained with tenside addition

The numerical solution of the PBE requires its discretization, which in the first step involves dividing the particles into a predefined number of diameter classes/cells, each of which containing a certain number of particles, N. After numerical determination of N corresponding to each class, this result can be converted to volume or number density distribution. Figure 11 shows a comparison of experimental and numerically determined particle numbers, N, in each discrete diameter class (Fig. 11a) and the corresponding volume density distributions, q_3 (Fig. 11b). The curves shown here were calculated by first fitting the model to the experimental data to obtain missing parameter β_0. The determined via optimization procedure value of aggregation rate of the

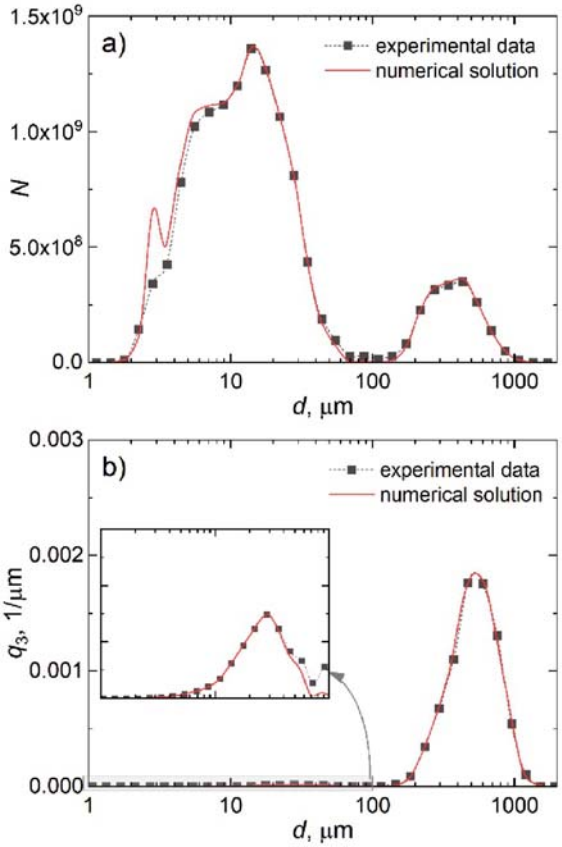

Figure 11. Comparison of experimental and numerically determined: (a) number of particles in each particle size class, N, and (b) volume density distribution, q_3

EKE kernel resulted to be $\beta_0 = 2.657 \cdot 10^{-12}$, with the corresponding value of the drain rate $K = 2.946 \cdot 10^{-4}$ 1/s. Interestingly, the obtained value β_0 is very close to that determined in previous work[5] for a process run in batch mode ($\beta_0 = 2.497 \cdot 10^{-12}$). Figure 11 demonstrates that, except for some inaccuracies in the small diameter range, the model based on PBE performs surprisingly well. This inaccuracy may be due to the assumptions made for the fines, i.e. neglecting nucleation from overspray or abrasion, or assuming a uniform probability of particle removal from the fluidized bed, including fines.

CONCLUSIONS

The study explores the influence of drying and granulation process conditions on the characteristics of micronutrient chelates granules. The process under investigation was carried out in a continuous mode in a pilot-scale FBSG installation. The facility used consisted of a fluidized bed apparatus with an external product separation system and a mill used to grind the oversize granules, which were then returned along with the dust to the fluidized bed.

The impact of the addition of surfactants to the fertilizer solution sprayed into the fluidized bed during the production of *N*-(1,2-dicarboxyethyl)-D,L-aspartic acid disodium zinc salt on the granules PSD and their morphology was analyzed. The influence of changing the mill rotational speed on the continuous granulation process was also examined. Experimental research was complemented by computational studies based on the PBE approach.

It was shown that granules produced with the addition of tensides in the continuous FBSG process have a more regular shape than granules obtained without tensides. As a result, they are less likely to suffer mechanical wear both during the process and later during transportation and storage of the product.

It was demonstrated that changing the rotor speed in the universal rotor mill affects the PSD and granule morphology without significantly disturbing the steady state. No dust deposits were observed on the granulator walls. However, an excess of seeds still helps to keep the process far from the so-called wet quenching, and the process air flow needs to be well-controlled. By using a higher rotor speed and, consequently, obtaining a higher mass air flow, the negative effect of dust accumulation is delayed or eliminated, thus preventing pipes from becoming clogged.

The results obtained from numerical solution of the population balance equation, indicate that, despite the relatively simple structure of the model, its use for predicting the operation of the apparatus or its control is still feasible. The advantage of the model employed is that it incorporates a limited number of parameters that can be fitted based on experimental results. The accuracy of the numerical results obtained in this study can undoubtedly be improved by incoropration additional nucleation mechanisms such overspray or attrition within the model. The same applies to a more accurate description of the mechanism for classifying granules withdrawn from the bed. However, these issues require additional work of both experimental and numerical nature and will be the subject of further research

ACKNOWLEDGMENTS

The research was carried out as part of an implementation PhD project. (Ministry of Science and Education, Poland)

LTERATURE CITED

1. Grünewald, G., Westhoff, B. & Kind, M. (2010). Fluidized bed spray granulation: nucleation studies with steady-state experiments. *Dry. Technol.* 28, 349–360. DOI: 10.1080/07373931003641495.

2. Rieck, C., Bück, A. & Tsotsas, E. (2020). Estimation of the dominant size enlargement mechanisms in spray fluidized bed process. *AIChE Jurnal* 66, e16920. DOI: 10.1002/aic.16920.

3. Iveson, S.M., Litster, J.D., Hapgood, K. & Ennis, B.J. (2001). Nucleation, growth and breakage phenomena in agitated wet granulation processes: a review. *Powder Technol*. 117, 3–39. DOI: 10.1016/S0032-5910(01)00313-8.

4. Burggraeve, A., Monteyne, T., Vervaet, C., Remon, J.P. & De Beer, T. (2013). Process analytical tools for monitoring, understanding, and control of pharmaceutical fluidized bed granulation: A review. *Eur. J. Pharm. Biopharm*. 83, 2–15. DOI: 10.1016/j.ejpb.2012.09.008.

5. Michałek, B., Ochowiak, M., Bizon, K., Włodarczak, S., Krupińska, A., Matuszak, M., Boroń, D., Gierczyk, B. & Olszewski, R. (2021). Effect of adding surfactants to a solution of fertilizer on the granulation process. *Energies* 14(22), 7557. DOI: 10.3390/en14227557.

6. Askarishahi, M., Maus, M., Schröder, D., Slade, D., Martinetz, M. & Jajcevic, D. (2020). Mechanistic modelling of fluid bed granulation, Part I: Agglomeration in pilot scale process. *Int. J. Pharm*. 573, 118837. DOI: 10.1016/j.ijpharm.2019.118837.

7. Askarishahi, M., Salehi, N.-S., Maus, M., Schröder, D., Slade, D. & Jajcevic, D. (2020). Mechanistic modelling of fluid bed granulation, Part II: Eased process development via degree of wetness. *Int. J. Pharm*. 572, 118836. DOI: 10.1016/j.ijpharm.2019.118836.

8. Saleh, K. & Guigon, P. (2007). Coating and encapsulation processes in powder technology. In Salman, A.D., Hounslow, M.J. & Seville, J.P.K. (Eds.), *Granulation* (pp. 323–375), Amsterdam, The Netherlands: Elsevier.

9. Lister, J. & Ennis, B. (2004). *The science and engineering of granulation processes.* Dordrecht, The Netherlands: Springer-Science+Business Media.

10. Kovalchuk, N.M., Simons, M.J.H. (2021). Surfactant-mediated wetting and spreading: Recent advances and applications. *Curr. Opin. Colloid Interface* 51, 101375. DOI: 10.1016/j.cocis.2020.07.004.

11. Januszkiewicz, K., Mrozek-Niećko, A. & Różański, J. (2019). Effect of surfactants and leaf surface morphology on the evaporation time and coverage area of ZnIDHA. *Plant Soil* 434, 93–105. DOI: 10.1007/s11104-018-3785-4.

12. Hemati, M., Cherif, R., Saleh, K., Pont, V. (2003). Fluidized bed coating and granulation: influence of process-related variables and physicochemical properties on the growth kinetics. *Powder Technol*. 130, 18–34. DOI: 10.1016/S0032-5910(02)00221-8.

13. Zank, J., Kind, M. & Schlünder, E.-U. (2001). Particle growth in a continuously operated fluidized bed granulator. *Dry. Technol*. 19, 1755–1772. DOI: 10.1081/DRT-100107271.

14. Kapur, P.C. & Fuerstenau D.W. (1969). Coalescence model for granulation. *Ind. Eng. Chem. Process Des. Dev*. 8, 56–62. DOI: 10.1021/i260029a010.

15. Breuer, M. & Almohammed, N. (2015). Modelling and simulation of particle agglomeration in turbulent flows using a hard-sphere model with deterministic collision detection and enhanced structure models. *Int. J. Multiph. Flow.* 73, 171–206. DOI: 10.1016/j.ijmultiphaseflow.2015.03.018.

16. PN-EN ISO7837-2000.

17. PN-EN ISO 845:2000.

18. ISO 12154:2014(E).

19. Hounslow, M.J., Ryall, R.L. & Marshall, V.R. (1988). A discretized population balance for nucleation, growth, and aggregation. *AIChE Jurnal* 34, 1821–1832. DOI: 10.1002/aic.690341108.

20. Vreman, A.W., Van Lare, C.E. & Hounslow, M.J. (2005). A basic population balance model for fluid bed spray granulation. *Chem. Eng. Sci*. 64, 4389–4398. DOI: 10.1016/j.ces.2009.07.010.

21. Otto, R., Dürr, R. & Kienle, A. (2023). Stability of combined continuous granulation and agglomeration processes in a fluidized bed with sieve-mill-recycle. *Processes* 11, 473. DOI: 10.3390/pr1102047.

22. Heinrich, S., Peglow, M., Ihlow, M., Henneberg, M. & Mörl, L. (2002). Analysis of the start-up process in continuous fluidized bed spray granulation by population balance modelling. *Chem. Eng. Sci*. 57, 4369–4390. DOI: 10.1016/S0009-2509(02)00352-4.

23. Hounslow, M.J. (1990). A discretized population balance for continuous systems at steady state. *AIChE J.*36, 106–116. DOI: 10.1002/aic.690360113.

24. Cronin, K., Ortiz, F.J., Ring, D. &Zhang, F. (2021). A new-time dependent rate constant of coalescence kernel for modelling of fluidized bed granulation. *Powder Technol.* 379, 321–334. DOI: 10.1016/j.powtec.2020.10.083.

25. Otto, E., Dürr, R., Strenzke, G., Palis, S., Bück, A., Tsotsas, E. & Kienle, A. (2021). Kernel identification in continuous fluidized bed spray agglomeration from steady state data. *Adv. Powder. Technol.* 32, 2517–2529. DOI: 10.1016/j.apt.2021.05.028.

26. Li, Z., Kessel, J., Grünewald, G., Kind, M. (2012). CFD simulation on drying and dust integration in fluidized bed spray granulation. *Dry. Technol.* 30, 1088–1098. DOI: 10.1080/07373937.2012.685672.